

Effects of Plasma Screening and Auger Recombination on the Luminescent Efficiency in GaP

K. P. SINHA AND M. DiDOMENICO, JR.

Bell Telephone Laboratories, Murray Hill, New Jersey 07974

(Received 15 September 1969)

A theoretical study of the concentration quenching of the luminescence in GaP is presented. The formulation takes cognizance of the effects of plasma screening on the electron- and hole-capture probability in forming bound excitons, and on various nonradiative (Auger) processes. For the system GaP(Zn,O), the luminescence is proportional to the branching ratio out of the exciton state given by $b = \{1 + (\tau_{xr}/\tau_{xn}) + [(1-f)/f](\tau_{xr}/\tau_{en})\}^{-1}$, where τ_{xr} and τ_{xn} are, respectively, the radiative and nonradiative (Auger) lifetimes of the bound excitons, τ_{en} is the Auger lifetime of bare trapped electrons, and f is an occupancy factor for the bound excitons. The f factor depends on the Fermi level, temperature, exciton capture probability, and τ_{xr} and τ_{xn} . The occupancy factor is found to be a sensitive function of doping. The exciton-capture probability is found to be proportional to $[1 + (q_s/\beta)]^{-8}$, where q_s is the screening parameter and β is reciprocal of the Bohr radius of the exciton. Thus the probability falls rapidly for $q_s \geq \beta$. The two Auger lifetimes are found to have the form $\tau_{xn} = (Bp)^{-1}$ and $\tau_{en} = (Cp^2)^{-1}$, where p is the hole concentration, and B and C are coefficients which are calculated in terms of the various binding and transition energies. The results of our calculations show that the branching ratio is close to unity in the low-doping region but falls rapidly when the acceptor concentration increases beyond 10^{18} cm^{-3} . These results are in agreement with experimental data.

I. INTRODUCTION

GALLIUM phosphide is an indirect-gap semiconductor with energy gap $E_g = 2.34 \text{ eV}$ at $T \approx 20^\circ\text{K}$, and is of particular interest from the standpoint of luminescent processes since it exhibits a number of below band-gap radiative transitions.¹ These include donor-acceptor pair recombination² and exciton recombination at both isoelectronic impurities^{3,4} and nearest-neighbor donor-acceptor complexes.⁵⁻⁷ In this paper we consider the excitonic recombination processes and attempt to explain the experimentally observed dependence of the luminescent efficiency on impurity concentration (doping). To do this we calculate how the radiative decay efficiency of bound excitons depends on majority carrier plasma screening and Auger de-excitation mechanisms. Other workers have attempted to explain the concentration quenching of exciton luminescence by invoking Auger mechanisms.^{6,8} However, the important effects of plasma screening were not considered.

We shall be concerned mainly with GaP doped with zinc and oxygen—GaP(Zn,O). The GaP(Zn,O) system gives luminescence in the red region ($\approx 1.8 \text{ eV}$) and is

associated with excitons bound to nearest-neighbor Zn-O complexes.^{5,6} The electrically neutral Zn-O complex is a deep electron trap ($\approx 300 \text{ meV}$) which, after trapping an electron, can capture a hole by Coulomb attraction into a shallow level ($\approx 36 \text{ meV}$). The quantum efficiency of the radiative excitonic decay process is quite efficient for Zn concentrations near 10^{18} cm^{-3} . Beyond this Zn concentration range the quantum efficiency rapidly decreases⁷ (for fixed O concentration). We show that this behavior can be explained in terms of a simple model for the recombination kinetics when the effects of plasma screening by free holes and Auger interactions are included.

II. THEORETICAL FORMULATION

To explain the concentration quenching of the luminescence in p -type GaP(Zn,O) three problems must be solved. The first relates to a description of the recombination kinetics, the second to the effects of majority carrier screening on capture rates of electrons and holes into various trap states, and the third to nonradiative Auger transitions. In our formulation we treat the excitons, either weakly or tightly bound, as independent particles and assume that the semiconductor consists of two simple parabolic bands, a valence and conduction band.

A. Recombination Kinetics

We consider first the steady-state recombination rates and radiative branching ratios for excitons based on a simple model of the recombination kinetics.⁹ The central process giving rise to bound excitons, after excess minority carriers have been generated either

¹ D. G. Thomas, in *Localized Excitations in Solids*, edited by R. F. Wallis (Plenum Press, Inc., New York, 1968).

² D. G. Thomas, M. Gershenson, and F. A. Trumbore, *Phys. Rev.* **133**, A269 (1964).

³ D. G. Thomas and J. J. Hopfield, *Phys. Rev.* **150**, 680 (1966).

⁴ F. A. Trumbore, M. Gershenson, and D. G. Thomas, *Appl. Phys. Letters* **9**, 4 (1966).

⁵ B. Welber, T. N. Morgan, and J. E. Scardefield, *Bull. Am. Phys. Soc.* **12**, 383 (1967); T. N. Morgan, B. Welber, and R. N. Bhargava, *Phys. Rev.* **166**, 751 (1968); C. H. Henry, P. J. Dean, and J. D. Cuthbert, *ibid.* **166**, 754 (1966).

⁶ J. D. Cuthbert, C. H. Henry, and P. J. Dean, *Phys. Rev.* **170**, 739 (1968).

⁷ M. Gershenson, F. A. Trumbore, R. M. Mikulyak, and M. Kowalchik, *J. Appl. Phys.* **36**, 1528 (1965); **37**, 483 (1966).

⁸ J. C. Tsang, P. J. Dean, and P. T. Landsberg, *Phys. Rev.* **173**, 814 (1968).

⁹ J. M. Dishman and M. DiDomenico, Jr., *Phys. Rev.* (to be published).

optically or by a forward biased p - n junction, is indicated illustratively in Fig. 1 for a p -type semiconductor. In our model electrons (holes) are trapped at an impurity or defect center as a first step. Subsequently, holes (electrons) are also trapped as weakly bound effective-mass particles thereby creating a bound exciton. The recombination process therefore involves the probability of capture of both particles at (charged) point defects, and the probability of radiative and nonradiative decay of the exciton.¹⁰ Capture probabilities and nonradiative Auger processes are treated below.

For definiteness we analyze the configuration shown in Fig. 1 and let the density of traps be N_t , the density of traps with electrons be N_{t^e} , the density of traps with excitons be N_{t^x} , and the density of traps with bare electrons be N_{t^-} . We define an occupancy factor f for bound excitons as

$$N_{t^x} = fN_{t^e}, \quad (1)$$

and note also that since $N_{t^e} = N_{t^x} + N_{t^-}$

$$N_{t^-} = (1-f)N_{t^e}. \quad (2)$$

Assuming that the electron-trap level is relatively deep compared to kT , the rate equation governing the exciton concentration is given by⁹

$$\dot{N}_{t^x} = (pN_{t^-}/\tau_{pt}N_t) - (p_hN_{t^x}/\tau_{pt}N_t) - (1/\tau_{xr} + 1/\tau_{xn})N_{t^x}, \quad (3)$$

where p denotes the concentration of holes, τ_{pt} is the lifetime for hole capture into the electron-occupied trap state, and τ_{xr} and τ_{xn} are, respectively, the radiative and nonradiative exciton lifetimes. The capture rate $1/\tau_{pt}$ can be written as

$$1/\tau_{pt} = v\sigma_{pt}N_t, \quad (4)$$

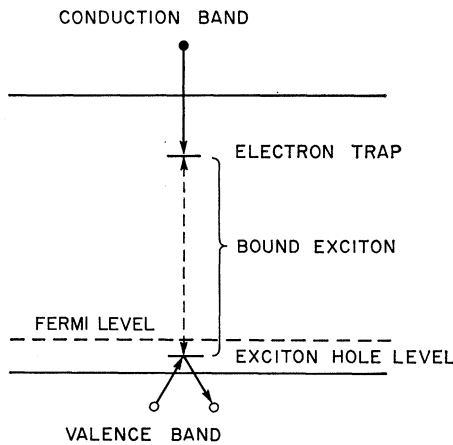


FIG. 1. Schematic diagram showing the trapping processes in the creation of bound excitons in a p -type semiconductor.

¹⁰ V. L. Bonch-Bruевич and E. G. Landsberg, Phys. Status Solidi 29, 9 (1968).

where v is the thermal velocity of holes and σ_{pt} is the thermally averaged hole-capture cross section. The second term in Eq. (3) describes the process of thermal emission of the hole bound in the shallow exciton hole level and can be evaluated at thermal equilibrium using detailed balance.⁹ The result is that the quantity p_h is given by

$$p_h = p e^{(E_f - E_h)/kT}, \quad (5)$$

where E_f is the Fermi level, E_h is the exciton-hole level (which includes the effects of screening as discussed below), and kT is the thermal energy. Combining Eqs. (1)–(3) we find in steady state ($\dot{N}_{t^x} = 0$) that the occupancy factor is given by

$$f = [1 + (p_h/p) + (\tau_{pt}N_t/p)(1/\tau_{xr} + 1/\tau_{xn})]^{-1}. \quad (6)$$

It is of interest to note that in the limit where $\tau_{pt}N_t(1/\tau_{xr} + 1/\tau_{xn}) \rightarrow 0$ the f factor reduces to the equilibrium Fermi factor for holes bound to the exciton hole level.

The quantum efficiency of the exciton recombination process may be expressed, in steady state, by a simple branching ratio b , i.e.,

$$b = \frac{N_{t^x}/\tau_{xr}}{N_{t^x}(1/\tau_{xr} + 1/\tau_{xn}) + N_{t^-}/\tau_{en}}, \quad (7)$$

where τ_{en} denotes the nonradiative Auger lifetime for trapped bare electrons. Using Eqs. (1) and (2) we then find

$$b = \{1 + (\tau_{xr}/\tau_{xn}) + [(1-f)/f](\tau_{xr}/\tau_{en})\}^{-1}. \quad (8)$$

We conclude that when $1/\tau_{en} \neq 0$, the exciton quantum efficiency becomes sensitive to the occupancy factor f . The f factor is in general a complicated function of doping owing to the effects of screening on the capture cross section σ_{pt} and the hole ionization energy E_h entering in Eq. (6) through the $\tau_{pt}N_t$ product and the p_h -factor, respectively. In the region of heavy doping, where the plasma screening length becomes comparable to the Bohr radius of the bound-hole, exciton formation becomes very improbable. This is reflected in a decrease in the f factor which, in turn, results in a reduction in the exciton quantum efficiency b .

B. Hole- (Electron-) Capture Cross Section

In our model (Fig. 1) electrons (holes) are deeply trapped at electrically neutral (Zn-O) defects. Holes (electrons) moving with thermal velocity can then be captured in s -like or p -like orbital states by the Coulomb potential of the resulting charged centers. We take for the interaction potential a screened Coulomb form given by

$$V = -(e^2/\epsilon r)e^{-q_s r}, \quad (9)$$

where r is the distance of the hole from the charged center, ϵ is the dielectric constant of the medium, e is electronic charge, and q_s is a screening parameter. Lax¹¹

¹¹ M. Lax, Phys. Rev. 119, 1502 (1960).

has calculated the capture cross section for a pure Coulomb potential ($-e^2/\epsilon r$) and shows that capture takes place by a multistep process in which a particle is initially captured into a shallow hydrogenic state followed subsequently by a cascading into the ground state with phonon emission. The cross section σ_{pt} can be written as

$$\sigma_{pt} = \int_0^{E_h} \sigma(U)P(U)dU, \quad (10)$$

where $\sigma(U)dU$ is the cross section for capture into a hydrogenic state with binding energy U , and $P(U)$ is the sticking probability for a state with binding energy U . Lax has shown that $\sigma(U)$ diverges as $1/U^{2.5}$ and $P(U)$ decreases approximately as $U^{3.5}$, so that the over-all dependence of σ_{pt} on binding energy E_h should be E_h^2 .

To calculate the dependence of σ_{pt} on the screening parameter q_s , we estimate the binding energy E_h in a hydrogenic state for pure Coulomb and screened Coulomb potentials. By making use of the relation $\sigma_{pt} \propto E_h^2$ we determine the functional form of the screening factor. The magnitude of the capture cross section in the unscreened case $\sigma_{pt}^0(q_s=0)$ must be calculated by the methods described by Lax.¹¹ We shall be concerned with s -like and p -like bound states, and for simplicity will consider specifically $1s$ and $2p$ states. It may be noted that these represent the total orbital functions of trapped electrons and holes and not the envelope functions. Using the virial theorem, the binding energy is half the potential energy which, in screened (E_h) and unscreened (E_h^0) cases, is given by

$$E_h^0 \propto \langle \varphi_{nl} | (e^2/\epsilon r) | \varphi_{nl} \rangle \propto (2\beta/n)^{-2(l+1)} \quad (11)$$

and

$$E_h \propto \langle \varphi_{nl} | (e^2/\epsilon r) \exp(-q_s r) | \varphi_{nl} \rangle \propto [(2\beta/n) + q_s]^{-2(l+1)}, \quad (12)$$

where φ_{nl} is the $1s$ and $2p$ hydrogenic wave function with quantum numbers n and l , and β is the reciprocal Bohr radius. From Eqs. (11) and (12) and the relation $\sigma_{pt} \propto E_h^2$ we find

$$\sigma_{pt} = \sigma_{pt}^0 [1 + (nq_s/2\beta)]^{-4(l+1)}. \quad (13)$$

For $1s$ and $2p$ states this reduces to

$$\sigma_{pt}(s) = \sigma_{pt}^0(s) [1 + (q_s/2\beta)]^{-4} \quad (14)$$

and

$$\sigma_{pt}(p) = \sigma_{pt}^0(p) [1 + (q_s/\beta)]^{-8}. \quad (15)$$

This predicts, as we might expect, that screening becomes important when $q_s \approx \beta$, and that σ_{pt} decreases rapidly in the region $q_s > \beta$. In the classical Debye limit we therefore conclude that screening affects the capture probability when the majority carrier concentration exceeds the critical value n_{crit} , where

$$n_{crit} = \epsilon k T / 4\pi e^2 a_0^2 \quad (16)$$

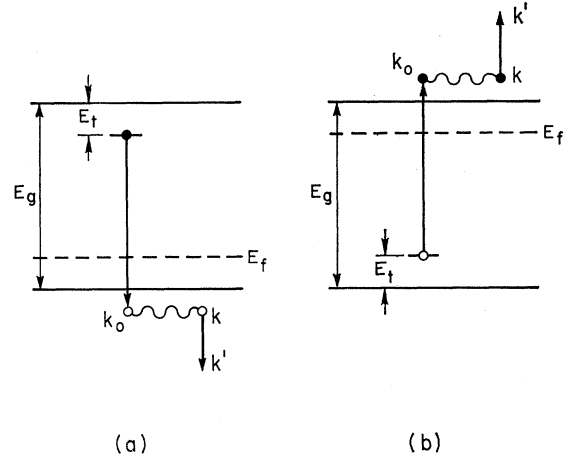


FIG. 2. Schematic representation of the Auger interactions of (a) trapped electrons in p -type and (b) trapped holes in n -type materials.

and a_0 is the Bohr radius. At room temperature this gives $n_{crit} \approx (\epsilon/a_0^2) \times 10^{20} \text{ cm}^{-3}$ when a_0 is in Angstrom units. Thus for $\epsilon \approx 10$ and $a_0 \sim 10\text{--}20 \text{ \AA}$, corresponding to binding energies of order 50 meV, we find $n_{crit} \sim 10^{18}\text{--}10^{19} \text{ cm}^{-3}$. We estimate therefore that in the doping range $10^{18}\text{--}10^{19} \text{ cm}^{-3}$ screening of the Coulomb capture cross section should become important.

C. Auger Recombination Lifetime

In this subsection we compute the radiationless recombination rate for several important Auger processes including explicitly the effects of screening. We distinguish between two basic processes: (1) recombination of trapped minority carrier electrons (holes) with majority carrier holes (electrons), and (2) recombination of excitons with free carriers. In Figs. 2 and 3 we outline diagrammatically some of the

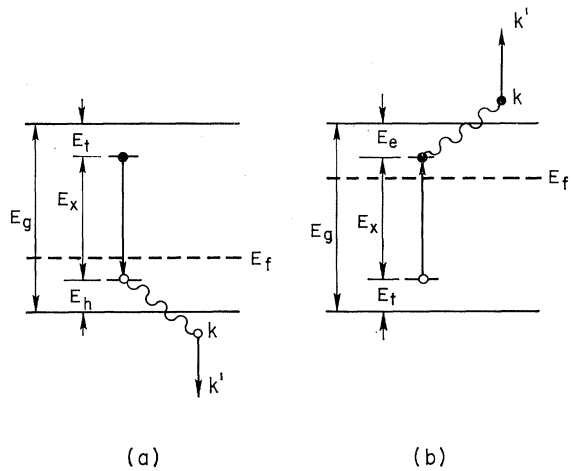


FIG. 3. Schematic representation of the Auger interactions of bound excitons in (a) p -type and (b) n -type materials.

important Auger processes. Other Auger processes exist (see Refs. 10 and 12 for a review of nonradiative processes); however, these involve exchange interactions between conduction-band electrons and valence-band holes and, as a consequence, are thought to be less probable than the processes indicated in Figs. 2 and 3. The interaction Hamiltonian H_{12} for any of the Auger processes is the electron-electron (or hole-hole) screened Coulomb interaction given by

$$H_{12} = (e^2/\epsilon r_{12})e^{-q_s r_{12}}, \quad (17)$$

where r_{12} is the relative distance between the two interacting particles.

1. Auger Recombination of Trapped Electrons (Holes)

To calculate the Auger lifetime of trapped electrons (holes) (see Fig. 2), we choose hydrogenic $1s$ wave functions for the trapped particles, i.e.,

$$\varphi_i = (\beta^3/\pi)^{1/2} e^{-\beta r}, \quad (18)$$

where β is the reciprocal Bohr radius. The wave functions of the free carriers are chosen to be plane waves of the form

$$\psi_k = (1/\Omega)^{1/2} e^{i\mathbf{k}\cdot\mathbf{r}}, \quad (19)$$

where Ω is the volume and \mathbf{k} is the wave vector. The matrix element for the processes shown in Fig. 2 is

$$\langle \varphi_i, \psi_{k'} | H_{12} | \psi_{k_0}, \psi_k \rangle = \frac{e^2(\beta^3/\pi)^{1/2}}{\epsilon\Omega^{3/2}} \iint \frac{d\mathbf{r}_1 d\mathbf{r}_2}{|\mathbf{r}_1 - \mathbf{r}_2|} \times e^{-q_s|\mathbf{r}_1 - \mathbf{r}_2| - \beta r_1 + i\mathbf{k}_0 \cdot \mathbf{r}_1 + i(\mathbf{k} - \mathbf{k}') \cdot \mathbf{r}_2}. \quad (20)$$

The type of integral in Eq. (20) has been evaluated by Bess.¹³ Using his results we obtain

$$\langle \varphi_i, \psi_{k'} | H_{12} | \psi_{k_0}, \psi_k \rangle = 32(e^2/\epsilon)(\pi/\Omega)^{3/2} \beta^{5/2} [q_s^2 + |\mathbf{k}_0 - \mathbf{k}'|^2]^{-1} \times [\beta^2 + |\mathbf{k} + \mathbf{k}_0 - \mathbf{k}'|^2]^{-2}. \quad (21)$$

The Auger transition rate $1/\tau_{en}$ appropriate for use in Eq. (3) is given by

$$1/\tau_{en} = \langle w_{en} \rangle p \Omega, \quad (22)$$

where $\langle w_{en} \rangle$ is the average transition probability and p is the hole (electron) concentration. The transition probability w_{en} is given by the familiar expression

$$w_{en} = (2\pi/\hbar)(\Omega/8\pi^3)^2 \iint d\mathbf{k}_i d\mathbf{k}_f |M_{if}|^2 \times \delta[E_i(\mathbf{k}) - E_f(\mathbf{k})], \quad (23)$$

where M_{if} is the initial-to-final-state matrix element in Eq. (21), $E_i(\mathbf{k})$ and $E_f(\mathbf{k})$ are the initial- and final-state energies, respectively, and the integration is over the

occupied initial states \mathbf{k}_i and the empty final states \mathbf{k}_f . Assuming that the energy bands are spherical and that for the situation shown in Fig. 2, $k' \gg k \approx k_0$, Eqs. (21) and (23) reduce to

$$w_{en} \approx (32e^2/\epsilon)^2 (\beta^5/2\hbar^3\Omega) (m^*/K) \int k^2 dk \times \int k'^2 dk' \frac{[\delta(k'+K) + \delta(k'-K)]}{(q_s^2 + k'^2)^2 (\beta^2 + k'^2)^4}, \quad (24)$$

in which

$$\hbar^2 K^2/2m^* = E_g - E_t, \quad (25)$$

where m^* is the effective mass, E_g is the energy gap, and E_t is the energy level of the trap (see Fig. 2). The average transition probability can be evaluated by using the approximation that the \mathbf{k} vectors of the initial states cut off at a value

$$k_e^3 \approx 6\pi^2 p, \quad (26)$$

where p is the valence-band hole (conduction-band electron) concentration. Using this approximation in Eq. (24) and substituting the result in Eq. (22) we find

$$\frac{1}{\tau_{en}} \approx \left(\frac{32\pi e^2}{\epsilon}\right)^2 \left(\frac{2m^*}{\hbar^3}\right) \frac{p^2 \beta^5 K}{(q_s^2 + K^2)^2 (\beta^2 + K^2)^4}. \quad (27)$$

It is convenient to recast this expression in a form which displays the dependence on free-carrier concentration and the energies E_g and E_t . To do this we relate the reciprocal Bohr radius β to the trap energy and the effective mass, i.e.,

$$\beta^2 = 2m^* E_t / \hbar^2. \quad (28)$$

Comparing Eqs. (25) and (28) we conclude that $K^2 \gg \beta^2$. In the Debye limit Eq. (27) then reduces to

$$\frac{1}{\tau_{en}} \approx \frac{1}{\hbar} \left(\frac{32\pi e^2}{\epsilon}\right)^2 \frac{E_t^{5/2} (E_g - E_t)^{1/2}}{E_g^4} \times \frac{p^2}{[(4\pi e^2 p / \epsilon k T) + 2m^* (E_g - E_t) / \hbar^2]^2}, \quad (29)$$

which differs, in certain respects, from the related expressions derived by others.^{10,12,13}

2. Auger Recombination of Bound Excitons

We now consider the Auger recombination of bound excitons. The interactions considered are shown in Fig. 3. For the sake of definiteness we treat the case of bound excitons in p -type crystals as shown in Fig. 3(a). We choose s -like wave functions for the trapped electrons and p -like wave functions for the trapped holes. These wave functions give allowed electric dipole transitions for the bound exciton. We denote the wave functions of the trapped minority carriers by φ_i and of the trapped majority carriers by Φ_i . The s states are

¹² P. T. Landsberg, in *Lectures in Theoretical Physics* (University of Colorado Press, Boulder, Colo., 1966), Vol. 8A.

¹³ L. Bess, *Phys. Rev.* **105**, 1469 (1957).

given by Eq. (18), and the p states are given by

$$\Phi_i(p) = (\beta^3/32\pi)^{1/2} \beta r \cos\theta e^{-\beta r/2}. \quad (30)$$

The matrix element for the interaction shown in Fig. 3(a) is

$$\begin{aligned} \langle \varphi_i, \psi_{k'} | H_{12} | \Phi_i, \psi_k \rangle \\ = \left(\frac{e^2}{\epsilon\Omega} \right) \left(\frac{\beta_n^3 \beta_p^3}{32\pi^2} \right)^{1/2} \iint \frac{d\mathbf{r}_1 d\mathbf{r}_2}{|\mathbf{r}_1 - \mathbf{r}_2|} \beta_p r_1 \cos\theta_1 \\ \times e^{-q_s |\mathbf{r}_1 - \mathbf{r}_2| + i(\mathbf{k} - \mathbf{k}') \cdot \mathbf{r}_2 - (\beta_n + \beta_p/2) r_1}, \quad (31) \end{aligned}$$

where β_n and β_p are, respectively, the reciprocal Bohr radii of electrons and holes. The matrix element can be evaluated straightforwardly and is given by

$$\begin{aligned} |\langle \varphi_i, \psi_{k'} | H_{12} | \Phi_i, \psi_k \rangle| = \left(\frac{32\pi e^2}{\sqrt{2}\epsilon\Omega} \right) (\beta_n \beta_p)^{3/2} \\ \times \left\{ \frac{\beta_p (\beta_n + \frac{1}{2}\beta_p) |\mathbf{k} - \mathbf{k}'|}{(q_s^2 + |\mathbf{k} - \mathbf{k}'|^2) [(\beta_n + \frac{1}{2}\beta_p)^2 + |\mathbf{k} - \mathbf{k}'|^2]^3} \right\}. \quad (32) \end{aligned}$$

The transition rate for Auger recombination of excitons $1/\tau_{xn}$ is given by Eq. (22) where the transition probability w_{xn} is now

$$\begin{aligned} w_{xn} = (2\pi/\hbar) (\Omega/8\pi^3) \\ \times \int d\mathbf{k}_f |M_{if}|^2 \delta[E_i(\mathbf{k}) - E_f(\mathbf{k})]. \quad (33) \end{aligned}$$

Substituting Eq. (32) into Eq. (33), performing the integration for spherical bands, and substituting the resulting expression for $\langle w_{xn} \rangle$ into Eq. (22) yields

$$\begin{aligned} \frac{1}{\tau_{xn}} = \left(\frac{32\pi e^2}{\epsilon} \right)^2 \left(\frac{2m^*}{\pi\hbar^3} \right) \\ \times \left\{ \frac{\beta_n^3 \beta_p^5 (\beta_n + \beta_p/2)^2 p K^3}{(q_s^2 + K^2)^2 [(\beta_n + \beta_p/2)^2 + K^2]^6} \right\}, \quad (34) \end{aligned}$$

where K is given by Eq. (25) with $E_g - E_t$ replaced by E_x the exciton recombination energy (see Fig. 3). We can convert Eq. (34) into a form which displays the dependence on free-carrier concentration and energy, as was done previously in Eq. (29), by making use of relations similar to Eq. (28). We assume for the configuration shown in Fig. 3(a) that the electron trap is deep so that $\beta_n \gg \beta_p$. This corresponds to the case of GaP(Zn,O). Taking an average effective mass m^* for both conduction and valence bands we find

$$\begin{aligned} \frac{1}{\tau_{xn}} = 32 \left(\frac{32\pi e^2}{\epsilon} \right)^2 \left(\frac{2m^*}{\hbar^2} \right)^{3/2} \left(\frac{E_x^{3/2} E_h^{5/2} E_t^{5/2}}{\pi\hbar E_g^6} \right) \\ \times \frac{p}{[(4\pi e^2 p / \epsilon kT) + 2m^* E_x / \hbar^2]^2}. \quad (35) \end{aligned}$$

That these expressions should involve the hole binding energy is to be expected. This will have important effects. A similar dependence does not occur in the results given elsewhere.⁸ These expressions apply equally well to an n -type crystal [Fig. 3(b)] if we replace p by n , E_h by E_e , the electron binding energy, and interpret E_t as a deep-hole trap.

3. Discussion of Screening Effects

In discussing the effects of screening we must distinguish between two interactions. The first is the screening of the basic electron-electron or hole-hole Coulomb interaction. This enters in the final expressions for the Auger recombination rates in Eqs. (29) and (35) as the factor $[(4\pi e^2 p / \epsilon kT) + 2m^* E_g / \hbar^2]^{-2}$. For typical semiconductors where $E_g \sim 1$ eV and $\epsilon \approx 10$ we find at room temperature that for $p < 10^{22}$ cm⁻³ screening of the basic electron-electron interaction is completely negligible. Thus we can simplify Eqs. (29) and (35) considerably by omitting the term $4\pi e^2 p / \epsilon kT$ in the denominator, i.e.,

$$\frac{1}{\tau_{en}} = A \left[\frac{E_t^{5/2}}{E_g^4 (E_g - E_t)^{3/2}} \right] p^2, \quad (36)$$

$$\frac{1}{\tau_{xn}} = 32 (A/\pi) (2m^*/\hbar^2)^{3/2} \left(\frac{E_h^{5/2} E_t^{5/2}}{E_g^6 E_x^{1/2}} \right) p, \quad (37)$$

where

$$A = (1/\hbar) (16\pi e^2 \hbar^2 / \epsilon m^*)^2. \quad (38)$$

The second and important screening interaction relates to the majority carrier screening of the Coulomb potential binding the electron and hole in the exciton. The shift in binding energy due to screening is given by¹⁴

$$E_h = E_h^0 - (2e^2/\pi\epsilon) q_s, \quad (39)$$

where q_s is the screening parameter, and E_h^0 is the binding energy at zero concentration. We expect that for deeply trapped electrons where $E_t \gg (2e^2/\pi\epsilon) q_s$ this screening effect will not be important. Therefore we conclude that the Auger process for bound electrons given by Eq. (36) will be largely independent of screening. However, the plasma screening shift has important repercussions for the Auger recombination of bound excitons because of the dependence on E_h in Eq. (37). These equations therefore suggest that in the Debye limit Auger recombination of bound excitons will only be important in the range

$$p \lesssim (3\epsilon kT/4\pi e^2) (\pi\epsilon E_h^0/2e^2)^2, \quad (40)$$

and that beyond this concentration limit the Auger mechanism for bound excitons will cut off despite the fact that $1/\tau_{xn}$ increases linearly with p . For typical binding energies $E_h^0 \sim 50$ meV we find from Eq. (40)

¹⁴ V. L. Bonch-Bruевич, Zh. Eksperim. i Teor. Fiz. **32**, 1092 (1957) [English transl.: Soviet Phys.—JETP **5**, 894 (1957)].

at room temperature that the cutoff concentration limit is $p_c \sim 10^{19} \text{ cm}^{-3}$ when $\epsilon \approx 10$. Below p_c bound excitons can form; above p_c bound excitons are no longer stable. This may appear to be an overstatement bearing in mind that the energy shift in Eq. (39) was derived by perturbation theory. There is no doubt, however, that there will be some binding-energy shift in the high-doping region. In our calculations we will use the weaker cutoff $E_h = E_h^0 - 10^{-8} p^{1/3} \text{ eV}$ as suggested by Bonch-Bruevich.¹⁴

III. APPLICATIONS TO GaP(Zn,O)

Using the results of the preceding analysis we now calculate the Zn concentration dependence of the quantum efficiency in GaP(Zn,O). The luminescent quantum efficiency η is given by the product of two branching ratios

$$\eta = sb, \quad (41)$$

where b is given by Eq. (8), and s is the rate of filling of the Zn-O electron trap compared to the net rate of decay of minority carriers out of the conduction band. In the limit where the processes competing for electron capture dominate⁹ (as in Zn, O-doped GaP), the s branching ratio is proportional to the product of the Zn concentration N_A and the oxygen concentration N_O , so that

$$\eta \propto b N_O N_A. \quad (42)$$

The b branching ratio [Eq. (8)] depends on the radiative exciton lifetime τ_{xr} , the Auger lifetimes τ_{xn} and τ_{en} , and the occupancy factor f . Combining Eqs. (5), (6), (15), and (43) we find for p -like exciton hole states that

$$f = \{1 + e^{(E_f - E_h)/kT} + (\tau_{pl}^0 N_i/p)[1 + (q_s/\beta)]^8 (1/\tau_{xr} + Bp)\}^{-1}, \quad (43)$$

in which $\tau_{pl}^0 N_i = 1/v\sigma_{pl}^0$, and B is the coefficient of p in Eq. (37).

In order to compute the concentration and temperature dependence of the occupancy factor f we examine separately each of the terms in Eq. (43). In a p -type crystal where the acceptor density N_A is much larger than the donor density N_D we can compute the Fermi level E_f from the relation¹⁵

$$e^{-E_f/kT} = 2(N_A/N_v) \times \{1 + [1 + 4(N_A/N_v)e^{E_A/kT}]^{1/2}\}^{-1}, \quad (44)$$

where E_A is the acceptor ionization energy and N_v is the density of valence-band state, i.e.,

$$N_v = 2(m^*kT/2\pi\hbar^2)^{3/2} = 4.831(m^*/m_0)^{3/2}T^{3/2} \times 10^{15} \text{ cm}^{-3}. \quad (45)$$

Here m_0 is the free-electron mass; in actual computation m^* is taken equal to m_0 . The Zn acceptor level E_A is

¹⁵ J. S. Blakemore, *Semiconductor Statistics* (Pergamon Publishing Corp., New York, 1962).

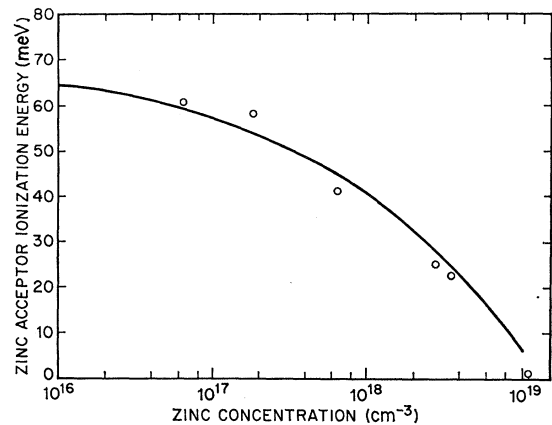


FIG. 4. Variation of zinc acceptor ionization energy versus zinc concentration in GaP(Zn,O). The full line is obtained from the empirical relation Eq. (46) with $E_A^0 \approx 71 \text{ meV}$. The open circles represent the experimental points of Casey *et al.* (Ref. 16).

known to shift with Zn concentration in GaP.¹⁶ Following the work of Pearson and Bardeen¹⁷ in Si and the work of Debye and Conwell¹⁸ in Ge, we use the following empirical relation for the concentration dependence of E_A :

$$E_A = E_A^0 - 3N_A^{1/3} \times 10^{-8} \text{ eV}. \quad (46)$$

In Fig. 4 we compare Eq. (46) with the experimental data of Casey *et al.*¹⁶ and find that the empirical relation is in excellent agreement with the data. Equation (46) appears to be related closely to the shift in binding energy due to screening given by Eq. (39). It is interesting to note that in the high-temperature limit where the hole density is approximately equal to the ionized acceptor concentration, Eq. (39) can be related to Eq. (46) by using the Thomas-Fermi screen-

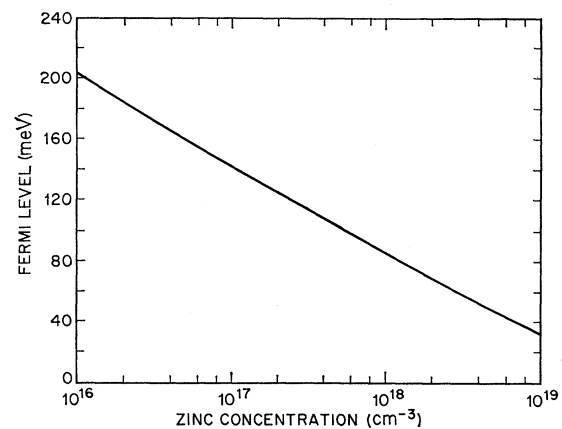


FIG. 5. Calculated values of the room-temperature (300°K) hole quasi-Fermi-level against zinc concentration in GaP(Zn,O). The sample is assumed to be uncompensated.

¹⁶ H. C. Casey, Jr., F. Ermanis, and K. B. Wolfstirn, *J. Appl. Phys.* **40**, 2945 (1969).

¹⁷ G. L. Pearson and J. Bardeen, *Phys. Rev.* **75**, 865 (1949).

¹⁸ P. P. Debye and E. M. Conwell, *Phys. Rev.* **93**, 693 (1954).

ing parameter $q_s = (3\pi^2 N_A)^{1/3}$. Room-temperature (300°K) values of E_f computed from Eqs. (44)–(46) are plotted in Fig. 5 as a function of Zn concentration.

The radiative lifetime of bound excitons τ_{xr} in GaP(Zn,O) is known to be about 10^{-7} sec.⁶ The electron occupied Zn-O center has a hole-capture cross section σ_{pi}^0 given by⁹

$$\sigma_{pi}^0 = 3.6 \times 10^{-16} T^{-1} \text{ cm}^2, \quad (47)$$

so that we estimate at $T = 300^\circ\text{K}$ $\tau_{pi}^0 N_i = 1/v\sigma_{pi}^0 \sim 10^{11} \text{ sec}^{-1} \text{ cm}^{-3}$. With $E_p \approx 2.2 \text{ eV}$, $E_t \approx 0.3 \text{ eV}$ and $E_h^0 \approx 0.036 \text{ eV}$ ($\beta = 4.6 \times 10^6 \text{ cm}^{-1}$), the Auger B coefficient for bound excitons, $1/\tau_{xn} = Bp$, obtained from Eq. (37), has the value

$$B \sim (E_h/E_h^0)^{5/2} \times 10^{-11} \text{ cm}^3/\text{sec}. \quad (48)$$

Substituting the parameters determined above into Eq. (43) with $p = N_s e^{-E_f/kT}$ and using Debye screening for q_s we can calculate the Zn-concentration dependence of the f occupancy factor. The results of the computation are shown in Fig. 6.

We observe from Fig. 6 that the occupancy factor f is small in the low-concentration region and increases with Zn concentration until it reaches a maximum at a concentration of about $4 \times 10^{17} \text{ cm}^{-3}$. Beyond this range f drops off rapidly. The initial increase in f is due to a reduction in the Fermi level as the doping level increases (see Fig. 5). As a result, the probability of binding holes on the exciton hole level at E_h initially increases. However, at the higher Zn concentrations (beyond $\sim 5 \times 10^{17} \text{ cm}^{-3}$) screening effects become increasingly important ($q_s \gtrsim \beta$) as well as Auger effects. As a consequence, the probability of hole capture decreases and

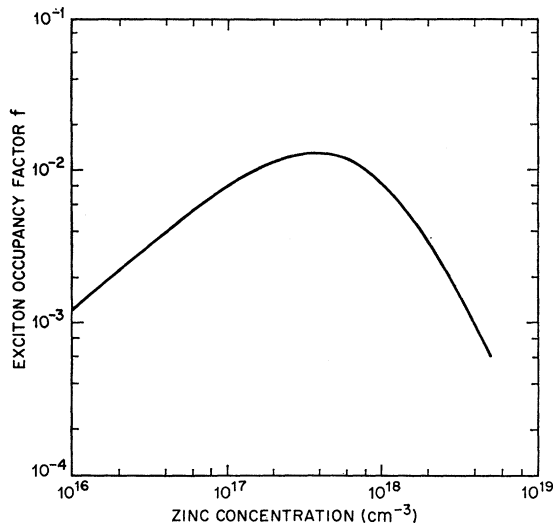


FIG. 6. Theoretical curve [cf. Eq. (43)] showing the room-temperature values of the exciton occupancy factor versus zinc concentration in GaP(Zn,O). The hole binding energy was computed from (Ref. 14) $E_h = E_h^0 - 10^{-8} p^{1/3} \text{ eV}$ with $E_h^0 \approx 0.036 \text{ eV}$. This expression was used for obtaining values of the reciprocal Bohr radius of the excitons and of the Auger B coefficient.

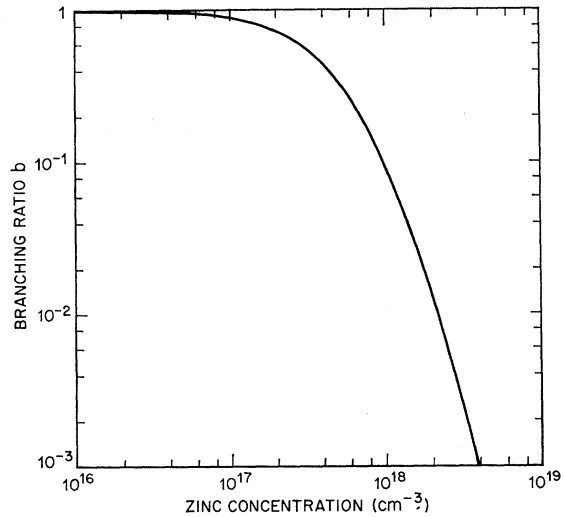


FIG. 7. Calculated behavior of the branching ratio b as a function of zinc concentration in GaP(Zn,O) at room temperature.

the probability of nonradiative exciton recombination increases causing f to drop off with increasing Zn concentration.

We next compute the concentration dependence of the b branching ratio given by Eq. (8). Using Eq. (36) to compute $1/\tau_{en}$, where $1/\tau_{en} = Cp^2$, and Eq. (37) to compute $1/\tau_{xn}$ we obtain from Eq. (8)

$$b = \{1 + \tau_{xr}[Bp + Cp^2(1-f)/f]\}^{-1}. \quad (49)$$

We can estimate the Auger C parameter as done previously for the B parameter and we find

$$C \sim 10^{-30} \text{ cm}^6/\text{sec}. \quad (50)$$

The concentration dependence of the branching ratio is shown in Fig. 7. In the low-concentration regime, the branching ratio remains close to unity; however, it falls off rapidly near and beyond an acceptor concentration of $N_A \sim 5 \times 10^{17} \text{ cm}^{-3}$. This is a consequence of the increase in free-carrier concentration which leads to a decrease in f (see Fig. 6) and a rapid increase of the two Auger terms contained in the square bracket of Eq. (49).

Figure 8 shows the dependence of the quantum efficiency η given by Eq. (42) on acceptor concentration. Also shown are room-temperature experimental data for the red Zn-O band in GaP. The theoretical and experimental results shown in Fig. 8 suggest that the red luminescence in GaP(Zn,O) quenches with Zn doping as a result of screening of the exciton binding energy and nonradiative Auger recombination processes. In the low-concentration region ($N_A < 10^{18} \text{ cm}^{-3}$) η is low because few Zn-O pairs form. As the Zn concentration increases the nearest-neighbor Zn-O pair concentration increases and η increases. Eventually, the acceptor concentration increases to the point where the b -branching ratio begins to decrease rapidly

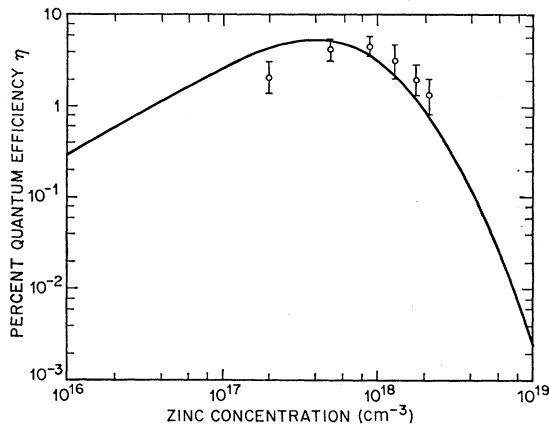


FIG. 8. Theoretical curve showing the zinc concentration dependence of the quantum efficiency ($\eta = sb$) in GaP(Zn,O) at room temperature. The experimental points were obtained for crystals grown with 0.02 mole% Ga₂O₃ in the melt.

($N_A > 5 \times 10^{17} \text{ cm}^{-3}$) with the result that η drops off with further increases in Zn concentration. The agreement between theory and experiment shown in Fig. 8 is good considering that an order-of-magnitude estimate was made for the various parameters. Better agreement can be obtained by adjusting the parameters determining the f occupancy factor and the Auger B and C coefficients.

IV. DISCUSSION

In the foregoing sections, we have presented a theoretical calculation of the luminescent efficiency of bound excitons in GaP as a function of doping. Although the calculations were developed for a specific system, i.e., GaP(Zn,O), they can be suitably adapted to other systems.

The determination of the luminescent efficiency is, in general, complex. The theoretical formulation involves the calculation of the probability of capture of carriers on point defects (leading to the formulation of bound excitons), and the probability of radiative and nonradiative decay processes. In our formulation we find that the quantum efficiency of the exciton recombination process is not a simple ratio of the probabilities of radiative and nonradiative decays. The present treatment shows that the efficiency is related to the branching ratio out of the exciton state which, in turn, depends on the radiative and nonradiative lifetimes as well as the exciton occupancy factor [cf. Eq. (8)]. The concept of the occupancy factor f is an important one. As seen from Eqs. (6) and (43) it depends on carrier concentration (and hence doping), the capture probability, the Fermi level, and the radiative and nonradiative exciton lifetimes. Thus it takes account of many detailed features of the recombination kinetics. Perhaps the most important information it contains is the effect of plasma screening,

which causes the capture lifetime to become longer in the high-doping region ($q_s \geq \beta$). This is demonstrated in Fig. 6 where the occupancy factor f falls sharply beyond the acceptor concentration of $\sim 5 \times 10^{17} \text{ cm}^{-3}$. Thus in this region the probability of formation of bound excitons falls rapidly owing to screening. This is reflected in the behavior of the branching ratio. The reason that the branching ratio remains close to unity in the low-doping region where f is very small is that the Auger terms Bp and Cp^2 are also very small. However, the low value of f in high-doping region augments the term $[(1-f)/f]Cp^2$ and the branching ratio falls rapidly, i.e., much faster than would be expected from a simple exciton Auger decay (Bp).

The fact that the over-all quantum efficiency in GaP(Zn,O) first increases with acceptor concentration and then falls for N_A beyond 10^{18} cm^{-3} is due to the behavior of the two branching ratios s and b in Eq. (41). In the low-concentration region b is close to unity but s increases with N_A . In the high-doping region b drops off much more rapidly than the linear increase in s . Thus the quantum efficiency reaches a maximum at a certain value of N_A beyond which it is quenched rapidly.

The present calculation can be extended to other systems exhibiting concentration quenching of the luminescence. We shall discuss briefly the results of the GaP(Bi,S) system. In this system bismuth acts as an isoelectronic trap. The electron-hole pairs produced in photoluminescent experiments are thought to follow the following capture sequence. The hole is first captured by a bismuth atom giving a Bi⁺ center in whose Coulomb field an electron is subsequently captured. The resulting excitons bind weakly to Bi ($\approx 100 \text{ meV}$) and give high quantum efficiency near band gap luminescence in the green region. Experimentally,⁸ it is found at low temperatures ($\sim 20^\circ\text{K}$) that the efficiency of the Bi luminescence is a rapidly decreasing function of the S donor concentration beyond a concentration of about 10^{18} cm^{-3} . Thermal quenching of the luminescence is observed to occur above 40°K with an activation energy of approximately 50 meV.

The situation in GaP(Bi,S) is very similar to that in GaP(Zn,O) except that the roles of electrons and holes are interchanged. There are a few important differences, however. The experimental results for GaP(Bi,S) are for much lower temperatures ($20^\circ \leq T \leq 100^\circ\text{K}$). Thus in the low-temperature ($\sim 20^\circ\text{K}$) and low-doping region the equilibrium concentration of conduction-band carriers may not exceed the optically generated carrier density. In this event,⁹ the exciton occupancy factor f will have the value $f \approx 1$. As the temperature increases, the Fermi level moves away from the bottom of the conduction band and carrier thermalization out of S donor levels will cause f to decrease. Thus, in the low-temperature and low-concentration domain, the branching ratio is given by

$b \approx (1 + \tau_{xr}/\tau_{xn})^{-1}$ with $1/\tau_{xn} \approx Bn$. The branching ratio is expected to remain close to unity until n increases with temperature to the point where τ_{xn} decreases. As a result, b will decrease with temperature. Owing to the fact that the binding energy E_t of holes at Bi is only about 40 meV,¹⁹ (unlike deep trapped electrons for the Zn, O case) the second branching ratio s becomes temperature-dependent. It involves a factor $[1 + \gamma e^{-E_t/kT}]^{-1}$, where γ is a dimensionless quantity weakly dependent on T . With increase in temperature s is expected to fall as a result of the low activation energy E_t . Thus the over-all quantum efficiency $\eta = sb$ quenches with temperature because both s and b fall.

The concentration quenching of the luminescence in the low-temperature (20°K) and high-doping region has been attributed by Tsang *et al.*⁸ to excitonic decay by an impurity-band Auger process. Although impurity banding does play an important role, one must also consider the role of plasma screening. From the work of Hara and Akasaki²⁰ there is experimental evidence that in sulfur-doped GaP, impurity banding sets in for an S concentration of $N_D \gtrsim 2 \times 10^{18} \text{ cm}^{-3}$. This is in good agreement with the estimate for the Mott transition.²¹ In the impurity-banding regime the probability of capture of electrons at the Bi⁺ centers will decrease owing to screening. Furthermore, the binding energy of the exciton electron may also shift [cf. Eq. (39)]. This may weaken the exciton Auger decay process; however, the delocalized electrons in the impurity band can still recombine with bare holes trapped at

Bi. The branching ratio is now given by

$$b = \{1 + \tau_{xr}[Bn + Cn^2(1-f)/f]\}^{-1}, \quad (51)$$

where n is to be regarded as the delocalized electron concentration. At the Mott transition, the occupancy factor has the value $f \approx \frac{1}{2}$ since the quasi-Fermi-level is close to the bottom of the conduction band. The Fermi level will, however, shift away from the conduction band with increasing temperature, making f much smaller. This and the fall in s with temperature may explain the further decrease of the branching ratio observed in the high-doping and high-temperature ($\sim 100^\circ\text{K}$) region. To obtain agreement with experimental results⁸ the B and C Auger coefficients are required to have larger values than for the GaP(Zn,O) system, i.e., $B \sim 10^{-8} \text{ cm}^3/\text{sec}$ and $C \sim 10^{-28} \text{ cm}^6/\text{sec}$. This value of B would be in accord with the estimate of Tsang *et al.*⁸ It would appear therefore that the presence of sulfur strengthens the Auger mechanism. A detailed comparison of our theoretical expression with experimental results is difficult, since a calculation requires knowledge of the dependence of n on N_D , the concentration dependence of E_f , the complicated role of sulfur electrons, and the effects of screening on binding energies and capture probabilities. If we make reasonable estimates for these parameters, we can get good agreement between the calculated concentration quenching and the observed quenching of the luminescence.

ACKNOWLEDGMENTS

The authors would like to thank M. L. Howe for assistance in the computer programming. We also thank R. Caruso for the experimental data in Fig. 8, and J. M. Dishman, R. A. Faulkner, and L. J. Varnerin for comments.

¹⁹ P. J. Dean, J. D. Cuthbert, and R. T. Lynch, Phys. Rev. **179**, 754 (1969).

²⁰ T. Hara and I. Akasaki, J. Appl. Phys. **39**, 285 (1968).

²¹ N. F. Mott, Phil. Mag. **6**, 287 (1961).